ELSEVIER

Journal of Molecular Catalysis A: Chemical 184 (2002) 379–386

JOURNAL OF MOLECULAR CATALYSIS A: CHEMICAL

www.elsevier.com/locate/molcata

Adsorption of sulfur on Ni_mB_2 clusters: a theoretical investigation on the mechanism of strong sulfur resistance of Ni–B alloy catalyst

Cheng Luo, Wen-Ning Wang, Ming-Hua Qiao, Kang-Nian Fan*

Laboratory of Molecular Catalysis and Innovative Materials, Department of Chemistry, Fudan University, Shanghai 200433, PR China

Received 10 July 2001; received in revised form 8 January 2002; accepted 22 January 2002

Abstract

Ni–B alloy is a novel industrial catalyst famous for its high activity, low-cost, and strong sulfur resistance in hydrogenation reactions. To get an insight into the special properties of Ni–B alloy catalyst, the adsorption of sulfur on Ni_mB_2 ($m = 1$–4) clusters has been studied with the density functional theory (DFT) method. The theoretical results show that the adsorbed sulfur tends to be connected with boron, not with nickel in the Ni–B alloy catalyst. This adsorption site prevents active nickel from being poisoned by sulfur or even being oxidized in the practical catalytic processes. This provides a sound explanation for the strong sulfur resistance of Ni–B alloy in the catalytic hydrogenation reactions.

Keywords: Ni–B alloy; Density functional theory; Sulfur resistance

1. Introduction

The effect of sulfur-containing molecules on the surfaces of metals or oxides has received a lot of attention recently [1–4]. This is partly motivated by the very negative effects of sulfur on the environmental protection and the industrial operations [5,6]. In the industrial catalytic processes, the sulfur impurities rapidly deactivate or poison most metal/oxide catalysts [7,8]. Two approaches are frequently followed to mitigate the negative effects of sulfur in the chemical industry. The first approach is to remove as much sulfur as possible from oil-derived feedstock using hydro-desulfurization catalysts and oxide sorbents [6,8]. The second approach is to improve the sulfur tolerance of catalytic processes currently used in industry by adopting catalysts that are less sensitive to sulfur poisoning [1,7,9–11]. The former approach is too complicated and costly to be practical in modern industry, and thus the second approach becomes the major preference for catalytic chemists who are seeking catalysts with high activity, low-cost, and strong sulfur resistibility.

Since 1980s, the metal–metalloid alloy catalysts have been extensively studied owing to their high catalytic activity, sharp selectivity and strong sulfur resistance in many liquid-phase hydrogenation reactions [12–15]. Among them, Ni–B and Ni–P alloy catalysts are most thoroughly studied [15–31]. Many experimental results and some models have been reported to elucidate the promoting effect of the alloying metalloid (B or P) on the catalytic activity. Wang et al. [27,28] reported that no significant decrease in the catalytic activity of $Ni–B/SiO_2$ catalyst was observed after a hydrogenation reaction for 1000 h

* Corresponding author. Fax: +86-21-6564-1740.
E-mail address: knfan@fudan.edu.cn (K.-N. Fan).

1381-1169/02/$ – see front matter
PII: S1381-1169(02)00037-7

in the presence of 10 ppm of sulfur. In contrast, the Ni/SiO_2 catalyst totally lost its activity within 24 h in the same circumstance. The weakening was also observed for the Ni–P/SiO_2 catalyst, and, even worse, the Ni–P/SiO_2 catalyst lost its activity immediately under the same reaction conditions, indicating its low sulfur resistibility. The above report demonstrated that Ni–B alloy catalyst has the superior sulfur resistibility. Imanaka et al. [32] and Nitta et al. [33] studied the poisoning effect on nickel and nickel–boride catalyst by a kinetic method, and reported that nickel–boride catalyst has strong sulfur resistibility in the hydrogenation reactions. The poisoning effect of carbon disulfide on Ni/SiO_2 or Ni–B/SiO_2 catalyst also has been studied in the past years. It have been concluded that sulfur interacts with nickel to form the surface or subsurface Ni_xS_y, which are inactive for the hydrogenation reaction. In order to understand how sulfur affects the structural, electronic, and chemical properties of Ni–B alloy catalyst, based on our previous works of the local structure of Ni–B alloy [34] which are quite in agreement with the results of experiments [35,36], in the present paper we will study the sulfur resistance mechanism of Ni–B alloy catalyst in the hydrogenation reactions with a series of Ni_mB_2S ($m = 1$–4) cluster models.

Two quantum chemistry methods were suggested in the field of solid-state research, i.e. the band structure calculation and the cluster model calculation. For the metallic glasses, the crystal periodicity is not preserved, and the local bonding is strengthened while the long-distance interaction is weakened. Thus it is reasonable to study the metallic glasses with the cluster model calculations. A suitable structure model of metal glasses is the key step to obtain a reasonable result, and it is necessary to understand the structure of the calculated object in order to model the solid-state correctly. It seems impossible to construct a simple cluster to model the complete structure for the metal glasses. The experimental data we have gotten about metal glasses till now are statistically averaged. Therefore, to understand the electronic properties of metal glasses in detail, the practical way is to choose a model that could correctly elucidate experimental facts. In the present paper, we adopt several Ni_mB_2 models, which will provide the results in agreement with the experimental data of Ni–B alloy and the sulfur resistance mechanism of Ni–B alloy in hydrogenation reactions.

2. Computational techniques and cluster modeling

Geometry optimization procedure was followed to determine the minimum-energy structure. Other properties were computed after the geometry had been optimized. The geometry of Ni_mB_2 clusters was fixed at the previous optimized geometry [34] when the position of the adsorbed sulfur atom is optimized.

All calculations were carried out by using the Gaussian 98 program package [37] with a Hartree–Fock (HF) and density functional theory (DFT) hybrid method, which is formed from Becke's three-parameter semi-empirical exchange function (Becke3) [38] along with the Lee, Yang, and Parr correlation function (LYP) [39,40]. The 18 core electron of nickel and sulfur were replaced by a relativistic effective core potential (RECP) generated by Hay and Wadt [41–43]. A (3s 3p 4d) primitive Gaussian basis set contracted to (2s 2p 2d) was used to represent the valance shell of the nickel and sulfur atom. A (9s 5p/3s 2p) basic set was used for boron [44].

In the present study, the Ni_mB_2S cluster models represent the adsorption of the sulfur atom on the Ni–B alloy catalyst. The reason why we choose the sulfur atom instead of other complicated sulfur-containing molecules to be the adsorbent is that on one hand, the sulfur atom is the simplest sulfur poison and can minimize the effect of surface metal atoms' being considerably reconstructed by the adsorption atoms or molecules, although the reconstruction of surface will have less effect on the adsorption energy [45] in catalytic reactions, and that on the other hand, Ni_mB_2 clusters have been proven to behave like the local structure of Ni–B alloys quite well by Fang et al. [34]. In the Ni_mB_2S cluster models, there exist two kinds of adsorption site: boron site and nickel site. The models in Fig. 1 are constructed according to the neutron diffraction findings that there exists boron–boron contact in the nickel–boron glass alloy.

3. Results and discussion

First, we optimize the adsorption site of the sulfur atom on the Ni_mB_2 clusters. The optimized geometry

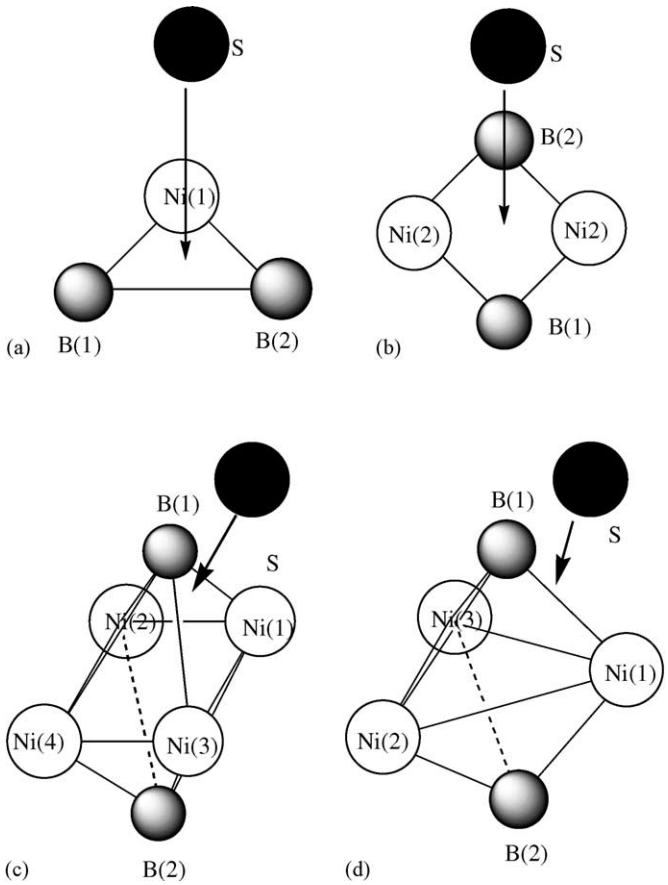

Fig. 1. Ni_mB_2S models: (a) NiB_2S; (b) Ni_2B_2S; (c) Ni_4B_2S; (d) Ni_3B_2S.

of Ni_mB_2S clusters, Mulliken population analyses and other calculation results are listed in Tables 1–4. As shown in Table 1, the bond distance of Ni–S (2.5617 Å for Ni_4B_2S and 2.3532 Å for Ni_3B_2S) is much longer than the summation of the covalent radii of sulfur atom and nickel atom ($r_{Ni} + r_S = 2.287$ Å), whereas the bond distance of S–B (1.8292 Å for Ni_4B_2S and 1.7673 Å for Ni_3B_2S) is shorter than the summation of the covalent radii of sulfur atom and boron atom ($r_S + r_B = 1.972$ Å). It is known that

Table 1
The optimized geometry of Ni_mB_2S ($m = 3$–4) clusters (bond length: Å)

	$R_{S-B(1)}$	$R_{S-B(2)}$	$R_{S-Ni(1)}$	$R_{S-Ni(2)}$	$R_{S-Ni(3)}$	$R_{S-Ni(4)}$
NiB_2S	1.9353	1.9353	3.4420			
Ni_2B_2S	2.3167	2.3167	2.6763	2.6763		
Ni_3B_2S	1.7673	3.4997	2.3532	3.6728	3.2935	
Ni_4B_2S	1.8292	3.2863	2.5617	3.6079	2.5617	3.6079
NiS			2.0501			
Ni_2S			2.1172	2.1172		

Table 2
The atomic charges of Ni_mB_2S ($m = 1$–4) clusters

	S	B(1)	B(2)	Ni(1)	Ni(2)	Ni(3)	Ni(4)
NiB_2S	0.021	0.010	0.010	−0.042			
Ni_2B_2S	−0.197	0.244	0.244	−0.146	−0.146		
Ni_3B_2S	−0.090	0.199	0.174	−0.128	−0.065	−0.089	
Ni_4B_2S	−0.145	0.279	0.071	−0.057	−0.045	−0.057	−0.045
NiS	−0.163			0.163			
Ni_2S	−0.074			0.037			

Table 3
The atom overlap population of Ni_mB_2S ($m = 3$–4) and Ni_mB_2 [34] clusters

	Ni_3B_2S	Ni_3B_2 [34]	Ni_4B_2S	Ni_4B_2 [34]
Ni(1)–Ni(2)	−0.121	0.0257	0.020	−0.1008
Ni(1)–Ni(3)	−0.005	0.0257	−0.195	−0.0465
Ni(1)–Ni(4)			−0.017	
Ni(2)–Ni(3)	0.059	−0.2081	−0.017	
Ni(2)–Ni(4)			−0.170	
Ni(3)–Ni(4)			0.020	
B(1)–B(2)	−0.157		−0.091	−0.0465
B(1)–Ni(1)	0.057	0.2141	0.036	0.1487
B(1)–Ni(2)	0.059	0.2407	0.099	
B(1)–Ni(3)	0.152	0.2141	0.036	
B(1)–Ni(4)			0.099	
B(2)–Ni(1)	0.295	0.2141	0.199	
B(2)–Ni(2)	0.188	0.2407	0.198	
B(2)–Ni(3)	0.223	0.2141	0.199	
B(2)–Ni(4)			0.198	
S–Ni(1)	0.205		0.149	
S–Ni(2)	−0.008		−0.007	
S–Ni(3)	0.014		0.149	
S–Ni(4)			−0.007	
S–B(1)	0.362		0.266	
S–B(2)	−0.019		−0.031	

the interaction between two atoms is stronger as its bond length is shorter. Sulfur atom prefers to combine with boron rather than with nickel in the modeling environment.

Table 4
The binding energy of Ni_mB_2S ($m = 3$–4) clusters model (kcal/mol)

	Full optimized	Near B site	Near Ni site
Ni_3B_2S	141.8	126.2	67.1
Ni_4B_2S	143.2	139.4	75.9
NiS	140.5		
Ni_2S	168.0		

The atomic charges of Ni_mB_2S ($m = 1$–4) are shown in Table 2. The average charge of Ni atoms in Ni_mB_2S ($m = 1$–4), compared with that in Ni_mB_2 is shown in Fig. 2. The adsorption of a sulfur atom, having higher electro-negativity, on Ni_mB_2 clusters reduces the quantity of negative charge on nickel atom significantly. However, the charge of nickel is still negative. Electron-rich nickel catalysts, such as Ni–B catalyst, are more effective and active than electron-deficient nickel catalysts, such as Ni–P catalysts [15]. In contrast, the charge of nickel is positive in Ni_mS(1–2) clusters in Table 2, which could be explained by considering that pure nickel is easy to combine with sulfur and lose its catalytic reactivity. Therefore, the existence of boron in Ni–B alloy catalyst leads to the retention of the electronic properties of catalyst. On the other hand, if sulfur connected to the metal atom, it would have altered the electronic properties of the metal [46–50] and consequently the metal catalyst would have lost its activity in catalytic processes.

According to overlap population analysis in Table 3, the interaction between nickel and boron atoms is strong. The interaction between the boron atoms themselves is in repulsion (anti-bonding). The unfavorable interaction between the boron atoms could be compensated by the favorable Ni–B interaction. These results are in agreement with the previous calculation [34] for the Ni_mB_2 models. Therefore, we can conclude that the adsorption of sulfur on Ni–B alloy hardly changes the electronic properties of nickel atoms, which is the active site of the catalyst. It further elucidates the reason why there exists strong sulfur resistance ability of nickel–boron alloy catalyst in hydrogenation reactions.

In order to compare the effect of sulfur adsorbed on different sites of nickel–boron alloy catalyst, two

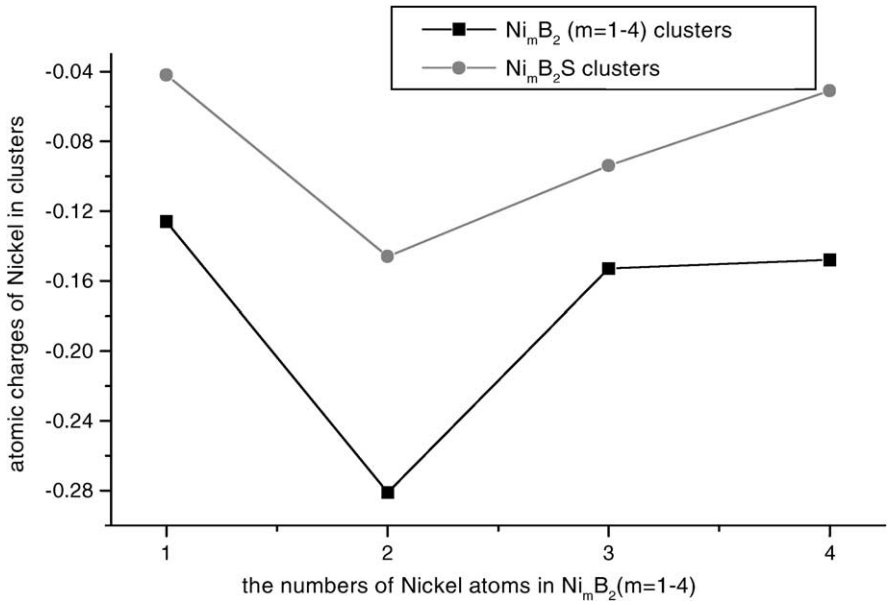

Fig. 2. The atomic charge of Ni_mB_2 [28] and Ni_mB_2S clusters.

additional models, sulfur adsorbed on near boron site and on near nickel site, are built and calculated. For the near boron site adsorption, the location of sulfur atom is optimized with the restriction that it is connected to the boron atom and along with the axis of boron–boron in the Ni_mB_2 clusters. For the near nickel site adsorption, the location of sulfur atom is optimized with the restriction that it is connected to the nickel atom and on the same plane of the nickel atoms. Both of the models are depicted in Fig. 3(a) and (b). The theoretical results are shown in Table 4.

As seen in Table 4, the binding energy of sulfur on nickel–boron alloy catalyst is substantial (141.8 kcal/mol for Ni_3B_2S and 143.2 kcal/mol for Ni_4B_2S). The adsorption energy of a sulfur atom on transition-metal surfaces varies between 80 and 140 kcal/mol [1]. The high adsorption energy of sulfur on Ni–B alloy catalyst is due to its low coordination. Table 4 also shows that the adsorption energies of sulfur atom on near boron site (126.2 kcal/mol for Ni_3B_2S, 139.4 kcal/mol for Ni_4B_2S) are similar to those of fully optimized clusters and pure nickel clusters (NiS and Ni_2S). Meanwhile, the adsorption of near nickel site has a much lower binding energy (67.1 kcal/mol for Ni_3B_2S and 75.9 kcal/mol for Ni_4B_2S). Therefore, we could confirm our previous view that when the sulfur-containing molecules are adsorbed on the Ni–B alloy catalyst, they prefer to combine with boron, instead of nickel. Thus their ability to poison the active nickel atoms decreases greatly. Consequently, Ni–B alloy catalyst is strongly resistant to sulfur in hydrogenation reactions.

It is well known that the activity of catalysis has a direct relation with its properties of electronic structure, especially the fermi level, the highest occupied molecular orbital (HOMO), and the lowest unoccupied molecular orbital (LUMO). In the present work we defined the fermi level to be the average value of HOMO and LUMO. Fig. 4 shows the energy level structure near fermi level in the Ni_4B_2S and Ni_4B_2 clusters. It shows that the fermi level of Ni_4B_2S (full optimization) and Ni_4B_2S (near boron site) is -4.025 and -4.007 eV, respectively, which is quite close to the previous theoretical Ni_4B_2 results (-4.110 eV) [34]. And the orbital distribution near the fermi level for the Ni_4B_2S (full optimization) and Ni_4B_2S (near boron site) clusters are also in good agreement with the previous theoretical Ni_4B_2

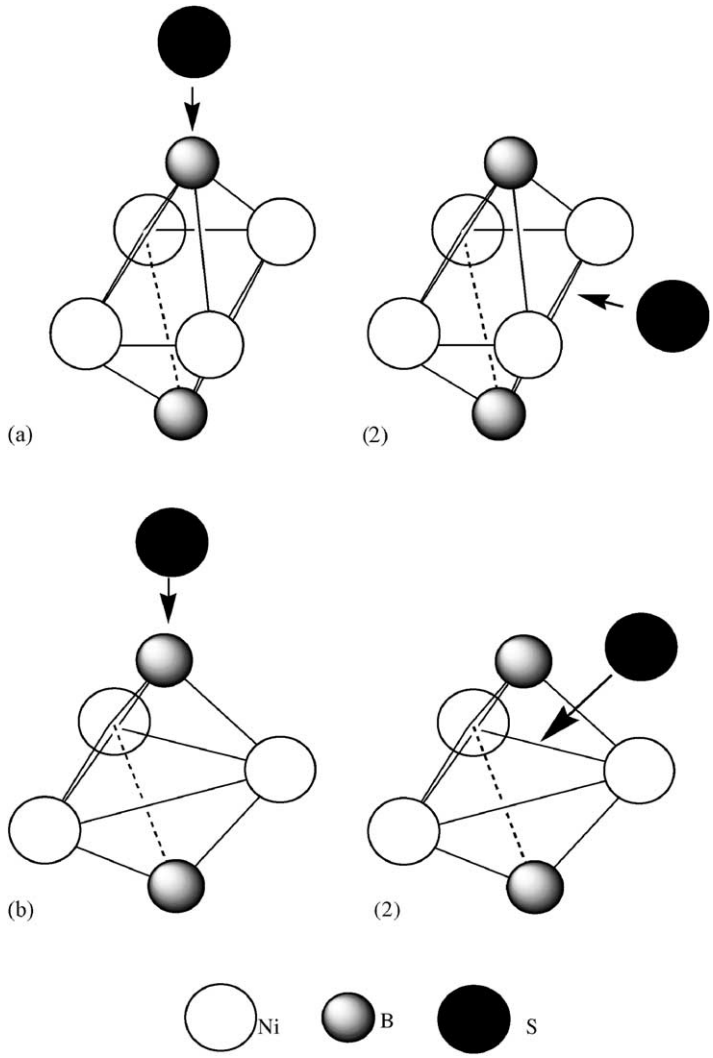

Fig. 3. Sulfur adsorbed on different sites of Ni_mB_2 clusters. (a) Ni_4B_2S: (1) near B site model, (2) near Ni site model; (b) Ni_3B_2: (1) near B site, (2) near Ni site.

results [34]. However, when the sulfur atom is adsorbed on the nickel site (see Fig. 3, near nickel site of Ni_4B_2S model), the fermi level and the orbital distribution change significantly. Furthermore, the results shown in Fig. 4 indicate that the fermi levels of Ni_4B_2S (full optimization), Ni_4B_2S (near boron site), and Ni_4B_2 are close to the average value of HOMO and LUMO of H_2 (−4.262 eV). Generally, transferring the electron from the HOMO of catalyst to the LUMO of hydrogen weakens the H–H bond in hydrogenation reactions. Therefore, the nickel–boron catalyst is still active after sulfur adsorbed. This explains the strong sulfur resistance of the nickel–boron alloy catalyst in hydrogenation reactions, which is in accordance with the observation about "Direct evidence for the anti-oxidation effect of boron on the ultra-fine amorphous Ni–B alloy catalyst" and the XPS experiments [51] whose boron is easily oxidized to form boron oxide in the surface layer of Ni–B alloy.

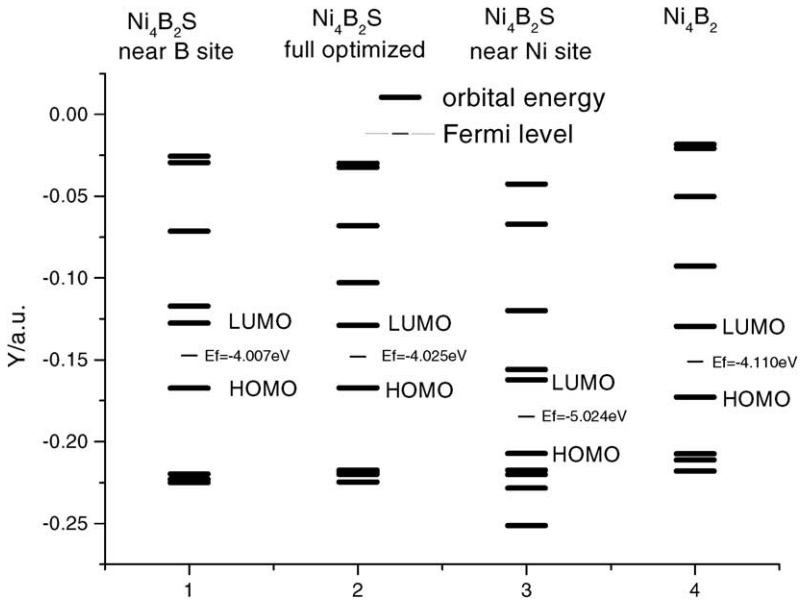

Fig. 4. Orbital distribution near fermi level of Ni_4B_2S and Ni_4B_2 [34] clusters.

4. Conclusion

The DFT results for the adsorption of sulfur (S) on the Ni_mB_2 clusters show that the near boron site in Ni–B alloy catalyst is preferable to combine with sulfur. The boron atoms in the Ni–B alloy catalyst are not only an electron-supplier to provide electron to nickel but also a defender to prevent Ni–B catalyst from being poisoned by the sulfur-containing molecules. Our theoretical work presents a sound elucidation for the strong sulfur resistance of the Ni–B alloy catalyst in the catalytic hydrogenation reactions.

Acknowledgements

This work was supported by the National Natural Science Foundation of China (No. 20073008 and No. 29892167) and Major State Basic Research Development Program (Grant No. G2000048009). CL thanks Dr. Yao-Ming Xie for helpful discussions.

References

[1] J.A. Rodriguez, J. Hrbek, Acc. Chem. Res. 32 (1999) 719.
[2] C.M. Friend, D.A. Chen, Polyhedron 16 (1997) 3165.
[3] B.C. Wiegand, C.M. Friend, Chem. Rev. 92 (1992) 491.
[4] J. Haase, J. Phys. 9 (1997) 3647.
[5] A.C. Stern, R.W. Boubel, D.B. Turner, D.L. Fox, Fundamentals of Air Pollution, 2nd Edition, Academic Press, Orlando, FL, 1984.
[6] J.M. Thomas, W.J. Thomas, Principles and Practice of Heterogeneous Catalysis, VCH, New York, 1997 (Chapter 6).
[7] J. Oudar, H. Wise, Deactivation and Poisoning of Catalysts, Dekker, New York, 1985.
[8] C.N. Satterfield, Heterogeneous Catalysis in Practice, McGraw-Hill, New York, 1980, pp. 259–265.
[9] K.C. Taylor, Catal. Rev. Sci. Eng. 35 (1993) 457.
[10] G. Ertl, H. Knozinger, J. Weitkamp, Handbook of Heterogeneous Catalysis, Wiley–VCH, New York, 1997.
[11] G. Somorjai, A Introduction to Surface Chemistry and Catalysis, Wiley, New York, 1994.
[12] Y. Chen, Catal. Today 44 (1998) 3.
[13] M. Shibata, T. Masumoto, Preparation of catalysts IV, in: B. Delmon, P. Grange, P.A. Jacobs, G. Poncelet (Eds.), Stud. Surf. Sci. Catal. 31 (1987) 353.
[14] A. Molnar, G.V. Smith, M. Bartok, Adv. Catal. 36 (1989) 329.
[15] H. Li, H.X. Li, W.L. Dai, W.J. Wang, Z.G. Fang, J.F. Deng, Appl. Surf. Sci. 152 (1999) 25.
[16] J.F. Deng, X.P. Zhang, Appl. Catal. 37 (1998) 339.
[17] J.F. Deng, X.P. Zhang, Solid State Ionics 32–33 (1989) 1006.
[18] J.F. Deng, H.Y. Chen, J. Mater. Sci. Lett. 12 (1993) 1508.
[19] J.F. Deng, J. Yang, S.S. Sheng, H.Y. Chen, G.X. Xiong, J. Catal. 150 (1994) 434.
[20] H.M. Wang, Z.B. Yu, H.Y. Chen, J. Yang, J.F. Deng, Appl. Catal. A 129 (1995) L143.

[21] W.L. Dai, M.-H. Qiao, J.F. Deng, Appl. Surf. Sci. 120 (1997) 119.
[22] Z.B. Yu, M.-H. Qiao, H.X. Li, J.F. Deng, Appl. Catal. A 163 (1997) 1.
[23] B.R. Shen, S. Wei, K.-N. Fang, J.F. Deng, Appl. Phys. A 65 (1997) 295.
[24] W.J. Wang, M.-H. Qiao, J. Yang, S.H. Xie, J.F. Deng, Appl. Catal. A 163 (1997) 101.
[25] H.X. Li, H.Y. Chen, S.Z. Dong, J.S. Yang, J.F. Deng, Appl. Surf. Sci. 125 (1998) 115.
[26] W.J. Wang, M.-H. Qiao, H.X. Li, J.F. Deng, J. Chem. Technol. Biotechnol. 72 (1998) 280.
[27] W.J. Wang, M.-H. Qiao, H.X. Li, J.F. Deng, Appl. Catal. A 166 (1998) L243.
[28] W.J. Wang, M.-H. Qiao, H.X. Li, W.L. Dai, J.F. Deng, Appl. Catal. A 168 (1998) 280.
[29] S.P. Lee, Y.W. Chen, Ind. Eng. Chem. Res. 38 (1999) 2548.
[30] S.P. Lee, Y.W. Chen, J. Mol. Catal. A 152 (2000) 213.
[31] S.P. Lee, Y.W. Chen, J. Chem. Technol. 75 (2000) 1073.
[32] T. Imanaka, Y. Nitta, S. Teranishi, Bull. Chem. Soc. Jpn. 46 (1973) 1134.
[33] Y. Nitta, T. Imanaka, S. Teranishi, Kogyo Kagaku Zasshi 74 (1971) 777.
[34] Z.G. Fang, B.R. Shen, K.-N. Fan, J.F. Deng, Acta Chim. Sin. 57 (1999) 894.
[35] A.M. Bratkovsky, A.V. Smirnov, J. Phys. 3 (1991) 5153.
[36] G.S. Chadha, N. Cowlaw, H.A. Davies, I.W. Donald, J. Non-Cryst. Solid 44 (1981) 265.
[37] M.J. Frisch, G.W. Trucks, H.B. Schlegel, G.E. Scuseria, M.A. Robb, J.R. Cheeseman, V.G. Zakrzewski, J.A. Montgomery Jr., R.E. Stratmann, J.C. Burant, S. Dapprich, J.M. Millam, A.D. Daniels, K.N. Kudin, M.C. Strain, O. Farkas, J. Tomasi, V. Barone, M. Cossi, R. Cammi, B. Mennucci, C. Pomelli, C. Adamo, S. Clifford, J. Ochterski, G.A. Petersson, P.Y. Ayala, Q. Cui, K. Morokuma, D.K. Malick, A.D. Rabuck, K. Raghavachari, J.B. Foresman, J. Cioslowski, J. V. Ortiz, B.B. Stefanov, G. Liu, A. Liashenko, P. Piskorz, I. Komaromi, R. Gomperts, R.L. Martin, D.J. Fox, T. Keith, M.A. Al-Laham, C.Y. Peng, A. Nanayakkara, C. Gonzalez, M. Challacombe, P.M.W. Gill, B. Johnson, W. Chen, M.W. Wong, J.L. Andres, C. Gonzalez, M. Head-Gordon, E.S. Replogle, J.A. Pople, Gaussian 98, Revision A.3, Gaussian Inc., Pittsburgh, PA, 1998.
[38] A.D. Becke, J. Chem. Phys. 98 (1993) 5648.
[39] C. Lee, W. Yang, R.G. Parr, Phys. Rev. B 37 (1988) 785.
[40] B. Miehlich, A. Savin, H. Stoll, H. Preuss, Chem. Phys. Lett. 157 (1989) 200.
[41] T.H. Dunning Jr., P.J. Hay, in: H.F. Schaefer III (Ed.), Modern Theoretical Chemistry, Vol. 3, Plenum Press, New York, 1976, p. 1.
[42] P.J. Hay, W.R. Wadt, J. Chem. Phys. 82 (1985) 270.
[43] W.R. Wadt, P.J. Hay, J. Chem. Phys. 82 (1985) 284.
[44] P.J. Hay, W.R. Wadt, J. Chem. Phys. 82 (1985) 299.
[45] B.R. Shen, Z.G. Fang, K.-N. Fan, J.F. Deng, Surf. Sci. 459 (2000) 206.
[46] J.A. Rodriguez, M. Kuhn, J. Hrbek, Surf. Chem. Phys. Lett. 251 (1996) 13.
[47] J.A. Rodriguez, S. Chaturvedi, T. Jirsak, Chem. Phys. Lett. 296 (1998) 421.
[48] P.J. Feibelman, D.R. Hamann, Surf. Sci. 149 (1985) 48.
[49] S. Wilke, M. Scheffler, Phys. Rev. Lett. 76 (1996) 3380.
[50] J.A. Rodriguez, M. Kuhn, J. Hrbek, J. Phys. Chem. 100 (1996) 3799.
[51] Y. Okamoto, Y. Nitta, T. Imanaka, S. Teranishi, J. Chem. Soc., Faraday Trans. 115 (1979) 2027.